ISSN 1063-7729, Astronomy Reports, 2007, Vol. 51, No. 10, pp. 797–807. © Pleiades Publishing, Ltd., 2007.
Original Russian Text © E.A. Koptelova, B.P. Artamonov, E.V. Shimanovskaya, V.V. Bruevich, A.S. Gusev, O.V. Ezhkova, 2007, published in Astronomicheskiĭ Zhurnal, 2007, Vol. 84, No. 10, pp. 885–895.

The Gravitational Lens Q2237+0305: Reduction and Analysis of the Observational Data

E. A. Koptelova, B. P. Artamonov, E. V. Shimanovskaya, V. V. Bruevich, A. S. Gusev, and O. V. Ezhkova

Sternberg Astronomical Institute, Moscow State University, Moscow, Russia

Received December 6, 2006; in final form, April 5, 2007

Abstract—The results of VRI photometry of the gravitationally lensed system Q2237+0305 carried out on the 1.5-m telescope of the Maidanak Observatory in 2004–2005 are presented. The method used to reduce the observational data is described in detail. An analysis of the brightness and color variations of the system's components is presented.

PACS numbers : 98.54.Aj, 95.75.De, 98.62.Sb
DOI: 10.1134/S1063772907100034

1. INTRODUCTION

Long-term monitoring data for gravitationally lensed systems can be used to study the most distant objects in the Universe: quasars and galaxies. The observed brightness variations for images of such a distant quasar, associated with both processes occurring in the source itself and with microlensing on the compact objects in the lensing galaxy, represent one of the main sources of information about the system.

Right from its discovery by Huchra et al. [1] in 1985, the gravitationally lensed system Q2237+0305, also known as the "Einstein Cross," began to be intensely investigated. Due to the high surface density and closeness of the lensing spiral galaxy ($z_l = 0.039$, a factor of 10 closer than the quasar itself, which has a redshift of $z_q = 1.695$), microlensing variations occur appreciably more often than in other known systems, including variations with high brightness amplification. In addition, the durations of events enable observations of microlensing activity over reasonable time intervals.

The first international project was carried out over three years on two different telescopes, with intervals between observations of slightly less than a year [2]. Starting in 1990, regular observations of the system in the V, R, and I filters were obtained over five years using the Nordic Optical Telescope (NOT) [3]. Data from the Gravitational Lens International Time Project (GLITP) monitoring group obtained from October 1999 through February 2000 became available in 2002 [4]. Regular V monitoring of Q2237+0305 by the Optical Gravitational Lens Experiment (OGLE) group was also begun in 1998. These monitoring data are distinguished by their high density and open availability. Regular observations of the system have been carried out using the 1.5-m telescope of the Maidanak Observatory since 1995. A large dataset in the V, R, and I filters has been obtained. The results of VRI photometry of the system for 1995–2000 were published in [5]. R light curves for the components based on observations obtained in 2002–2003 are presented in [6].

The observational material accumulated by the various groups clearly demonstrates that substantial, uncorrelated brightness variations of the system's components occur on time scales from several months to several years. Several microlensing events with high brightness amplifications have been identified in the system. Based on only two nights of observations (August 18 and September 16, 1988), Irwin and Webster [7] presented the first evidence for microlensing with high-amplification of component A. The generalized light curves constructed by Corrigan [2] using observations of several groups obtained during the summer and fall of 1988 confirmed this result. The variability amplitude was 0.16^m, and the duration of the event about 100 days. Two high-amplification microlensing events in components A and C were observed in 1999. The 1999 microlensing event for component C was accompanied by an increase in its R brightness by 1^m and a change in its $V-I$ color index by 0.42^m. During the 1999 microlensing event for component A, the R brightness increased by 0.45^m and the $V-I$ color index varied by 0.15^m. These events were observed by the OGLE group in V [8, 9] and the GLITP group in V filter [8, 9] and also by the GLITP group in V and R filters [4]. The

Table 1. I, R, V magnitudes of reference stars α and β according to the data of [2]

Star	I	R	V
α	17.26	17.28	17.50
β	17.70	17.83	18.18

resulting data are characterized by their high quality and high density.

Simultaneous with these observations, methods for the photometric reduction of data for the system have been developed [3, 10–14]. The choice of a particular method is dictated by the observing conditions, quality of the observational material, and the required accuracy for the photometric and astrometric characteristics of the system. In the current paper, we present data obtained during our monitoring of the Q2237+0203 system in 2004–2005, reduced using the method presented in [6, 15].

2. OBSERVATIONS AND PRELIMINARY REDUCTION OF THE DATA

Our observational data were obtained on the 1.5-m telescope of the Maidanak Observatory from June 2004 through November 2005. The system was observed in the V, R, and I filters using a CCD array mounted at the short (1 : 8) focus of the telescope. In addition to the target, the images contain three comparison stars (α, β, γ), whose magnitudes were measured using independent methods [2, 10]. The magnitudes for comparison star α and the reference star β are presented in Table 1. The exposure time did not exceed three minutes.

We used the Munich Image Data Analysis System (MIDAS) package for the preliminary reduction of the data, which included bias subtraction, flat-field correction using a flat field frame with a high signal-to-noise ratio, subtraction of the sky background, and removal of cosmic-ray traces. The small dark current due to the low operational temperature of the CCD camera avoids the need to subtract dark frames as part of the preliminary data reduction. We extracted a 64×64 pixel frame from the initial image ($17.1'' \times 17.1''$), centered on the nucleus of the lensing galaxy.

3. PHOTOMETRY OF THE OBSERVATIONAL DATA

A model image extracted from a CCD array mounted on a ground-based telescope is usually described by the convolution equation

$$t(i,j) * z(i,j) = u(i,j), \qquad (1)$$

where i and j are the pixel coordinates, $z(i,j)$ is the unknown brightness distribution, $t(i,j)$ is the point spread function (PSF), and $u(i,j)$ is the observed brightness distribution. Photometric measurements reduce to the task of finding the most complete description of the input image $z(i,j)$ based on the observed, blurred image $u(i,j)$ and the specified PSF $t(i,j)$.

Photometry of the components of the Q2237+0305 system is hindered by a number of factors. The distance between the components is of the order of $1''$, comparable with the full-width at half maximum (FWHM) of the point-source response. Even in good-quality images, the wings of the brightness distributions of the components overlap. The FWHM of the PSF is not constant during the observational season, and varies, on average, in the range $0.8''$–$2.0''$. The small distance between the system's components, the presence of the bright nucleus of the galaxy, and blurring due to the limited resolution of the instrumentation used and turbulence in the atmosphere lead to an overlap of the fluxes of components. Aperture-photometry methods, which can be used in regions with a low concentration of star-like sources and a uniform flat background, are not appropriate in the case at hand.

The model of the desired brightness distribution $z(i,j)$ in (1) can be represented as a sum of the point-like quasar components (four δ functions) and the brightness distribution of the lensing galaxy $g(i,j)$:

$$z(i,j) = \sum_{k=1}^{4} I_k \delta(i - x_k, j - y_k) + g(i,j), \qquad (2)$$

where δ denotes a Dirac δ function. The sum is carried out over the set of point sources with coordinates (x_k, y_k) and intensities I_k. The coordinates of the quasar components (x_k, y_k), their intensities I_k, and the brightness distribution of the galaxy $g(i,j)$ are unknown. Even if we do not take into account the presence of the non-uniform contribution of the galaxy (the $g(i,j)$ term in (2)), deriving accurate positions and intensities for the components is a very complex task. One possible general strategy is to obtain a model for the underlying galaxy, then derive the positions and intensities of the components. In this case, the accuracy of astrometric measurements will appreciably influence the final result obtained.

The presence of the bright galaxy and the various approaches used to describe this galaxy and take it into account in photometric measurements are one source of discrepancies between the results obtained by different monitoring programs, as well as discrepancies in the photometric results obtained by applying different methods to the same dataset [4, 11]. Determining the relative contributions of the point sources

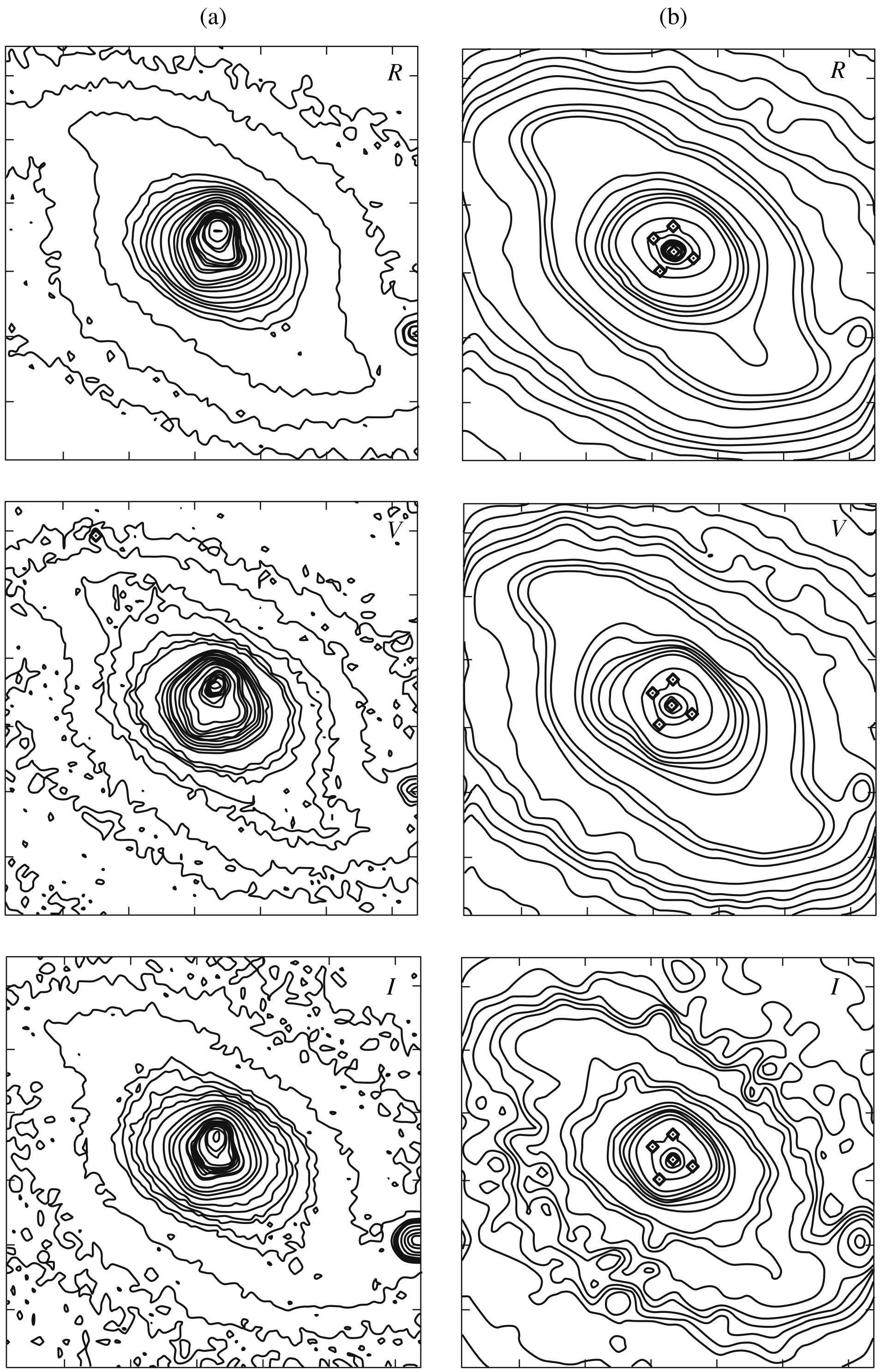

Fig. 1. Contours of equal R, V, I brightness for the (a) initial image of Q2237+0305 and (b) the reconstructed image free of the effects of the PSF. The size of the frame is 64×64 pixels ($17.1'' \times 17.1''$).

and galaxy in a resulting image is an important problem encountered in the photometric reduction of such a system.

Analytical [3–5] or numerical [10, 11] models are usually used to describe the brightness distribution of the galaxy. One advantage of using an analytical model is the appreciably smaller number of unknown parameters involved, which substantially shortens the

Table 2. R, V, I magnitudes of the lensing galaxy from the data of [20] in a $18.2'' \times 18.2''$ and based on observations with the Maidanak Observatory telescope in a $17.1'' \times 17.1''$ aperture

Telescope	R	V	I
NOT	15.10 ± 0.03	15.53 ± 0.04	14.87 ± 0.03
Maidanak	14.61 ± 0.08	15.03 ± 0.09	14.24 ± 0.06

computation times required. Reducing of the computation time is especially important when processing large datasets obtained during monitoring programs. However, it is difficult to describe the brightness distribution of a spiral galaxy with a bar using an analytical model. Using an inadequate model for the galaxy, in turn, leads to systematic errors in the photometry of the quasar components.

Determining a numerical model for the galaxy is an independent task. Numerical descriptions of the galaxy were used in [7, 10], and also in [2] to construct the first generalized light curves for the quasar components. In the method described in [10], the quasar components are successively subtracted and the galaxy image smoothed, after which the resulting model for the galaxy is used in photometry of the quasar components. A more complex procedure was applied in [2, 7]. First, the quasar components were removed via filtration and interpolation based on RB images of Q2237+0305, then numerical models for the bulge, bar, and spiral arms of the galaxy were constructed. The application of the algorithm described in [11] to carry out photometry of the components of Q2237+0305 was investigated by Belokurov et al. [16]. However, applying this method, which is based on regularization theory, to each individual frame obtained with exposure time of 3 minutes is hindered by the low signal-to-noise ratios of each frame. In addition, as was shown in [17, 18], the most stable results are obtained if it is assumed that the brightness distribution in the galaxy is close to a model profile. The algorithm described in [15] was used to search for a numerical model for the galaxy using an image obtained by averaging frames with seeing $\sim 0.8''$. Adding and averaging of frames was carried out to increase the signal-to-noise ratio. Figure 1 shows R, V, and I contours for the input image of the object and the reconstructed image that is free of the effects of the PSF.

The task of searching for numerical models for the galaxy involves a large number of free parameters (in our case, there were 4108 free parameters for the 64×64 reduced image). Applying an algorithm to photometrically process monitoring data would require excessive computational time. Since the galaxy makes a constant contribution to the component intensities, the frame-reduction procedure can be optimized by subtracting the contribution of the galaxy, assuming that it is constant from frame to frame. Thus, the same known galactic brightness distribution can be used to reduce each individual frame in order to derive astrometric and photometric parameters of the gravitationally lensed system. Since the signal and background levels change from frame to frame, in general, the galaxy's brightness distribution can be written

$$G(i,j) = \lambda_1 g(i,j) + \lambda_2, \tag{3}$$

where the coefficient λ_1 specifies the intensity of the galaxy in each frame and λ_2 the background. The algorithm is described and compared with the iterative CLEAN method [19] in [15], and was applied to monitoring data in [6]. In this formulation, the parameter λ_1 can be used to determine the apparent magnitude of the galaxy. Since we are using data for a fixed frame size for our reduction (64×64) and galaxy has the same brightness in all frames, constancy of the flux from the galaxy in the given aperture from frame to frame is a good test of the algorithm. Small fluctuations (to several per cent) can come about due to differences in the observing conditions. Table 2 presents the R, V, and I magnitudes of the lensing galaxy for the data of [20] obtained in a $18.2'' \times 18.2''$ aperture and for our own data obtained in a $17.1'' \times 17.1''$ aperture.

Realization of the photometric-reduction algorithm requires preliminary preparation of the observational data. Both images—the numerical model of the galaxy and the images of the system—must be brought into a unified coordinate system with the center of the numerical model shifted to the center of the galaxy in the frame being reduced.

4. RESULTS OF VRI PHOTOMETRY

Table 3 presents the results of our V photometry of the system components. The $V-R$ and $V-I$ color indices of the components are given in Tables 4 and 5. The resulting V light curves are shown in Fig. 2, compared to the OGLE data for the same observing period. For clarity of presentation, the light curves for components B, C, and D are shifted along the vertical axis by -0.3^m, 0.4^m, and 0.9^m, respectively. Figure 2 also shows the light curve of the comparison star α relative to the brightness of the reference star β ($\Delta m = m_\beta - m_\alpha$). The photometric results were calibrated using α (Table 1). Since α is near the target on the sky, we took no further action to take into account the effects of atmospheric extinction and airmass variations. Since the object was observed in series of 6–10 frames, we determined the errors in the

Table 3. V photometry of Q2237 + 0305 for the 2004–2005 Maidanak Observatory data (Julian date, the FWHM characterizing the seeing, and magnitudes for the four quasar components

JD-2450000	FWHM	A	B	C	D
53 163.0	$1.3''$	17.175 ± 0.005	18.583 ± 0.038	18.165 ± 0.015	18.322 ± 0.019
53 164.0	2.4	17.178 ± 0.006	18.531 ± 0.033	18.081 ± 0.014	18.249 ± 0.024
53 167.0	1.2	17.177 ± 0.006	18.536 ± 0.028	18.104 ± 0.013	18.278 ± 0.018
53 168.0	1.2	17.173 ± 0.006	18.437 ± 0.026	18.121 ± 0.014	18.322 ± 0.022
53 169.0	1.1	17.168 ± 0.005	18.524 ± 0.030	18.092 ± 0.012	18.356 ± 0.019
53 171.0	1.7	17.176 ± 0.006	18.575 ± 0.042	18.086 ± 0.017	18.412 ± 0.025
53 172.0	1.1	17.237 ± 0.004	18.546 ± 0.027	18.210 ± 0.011	18.395 ± 0.019
53 173.0	1.1	17.239 ± 0.005	18.557 ± 0.029	18.238 ± 0.011	18.344 ± 0.018
53 176.0	1.1	17.177 ± 0.005	18.515 ± 0.030	18.160 ± 0.012	18.379 ± 0.021
53 178.0	1.2	17.178 ± 0.006	18.534 ± 0.032	18.098 ± 0.015	18.348 ± 0.022
53 188.0	1.0	17.235 ± 0.005	18.554 ± 0.029	18.211 ± 0.013	18.361 ± 0.019
53 190.0	1.2	17.232 ± 0.004	18.554 ± 0.031	18.245 ± 0.015	18.397 ± 0.021
53 195.0	0.9	17.263 ± 0.007	18.555 ± 0.026	18.223 ± 0.011	18.324 ± 0.017
53 196.0	0.9	17.294 ± 0.004	18.528 ± 0.023	18.246 ± 0.011	18.372 ± 0.015
53 205.0	1.2	17.126 ± 0.006	18.541 ± 0.035	18.042 ± 0.015	18.313 ± 0.022
53 207.0	1.3	17.128 ± 0.005	18.571 ± 0.032	18.077 ± 0.013	18.210 ± 0.019
53 208.0	1.0	17.247 ± 0.009	18.525 ± 0.025	18.210 ± 0.012	18.338 ± 0.017
53 209.0	0.8	17.232 ± 0.006	18.575 ± 0.022	18.199 ± 0.011	18.496 ± 0.016
53 213.0	1.0	17.228 ± 0.005	18.527 ± 0.026	18.214 ± 0.013	18.398 ± 0.018
53 214.0	1.0	17.195 ± 0.004	18.511 ± 0.025	18.178 ± 0.014	18.295 ± 0.017
53 215.0	1.2	17.141 ± 0.005	18.533 ± 0.031	18.133 ± 0.013	18.295 ± 0.019
53 216.0	1.4	17.129 ± 0.007	18.561 ± 0.035	18.138 ± 0.015	18.288 ± 0.022
53 221.0	1.2	17.197 ± 0.005	18.507 ± 0.028	18.149 ± 0.014	18.182 ± 0.018
53 222.0	1.1	17.204 ± 0.005	18.550 ± 0.027	18.231 ± 0.013	18.309 ± 0.016
53 224.0	1.1	17.197 ± 0.006	18.555 ± 0.026	18.211 ± 0.012	18.329 ± 0.017
53 226.0	1.2	17.157 ± 0.007	18.478 ± 0.031	18.115 ± 0.015	18.273 ± 0.019
53 227.0	1.1	17.183 ± 0.006	18.504 ± 0.028	18.164 ± 0.013	18.336 ± 0.019
53 230.0	1.0	17.178 ± 0.005	18.455 ± 0.025	18.197 ± 0.012	18.296 ± 0.017
53 231.0	1.1	17.194 ± 0.006	18.428 ± 0.028	18.192 ± 0.013	18.307 ± 0.019
53 232.0	1.3	17.183 ± 0.008	18.493 ± 0.034	18.004 ± 0.016	18.258 ± 0.021
53 234.0	1.2	17.115 ± 0.006	18.480 ± 0.029	18.113 ± 0.014	18.286 ± 0.021
53 235.0	1.1	17.130 ± 0.005	18.501 ± 0.028	18.162 ± 0.013	18.203 ± 0.017
53 237.0	1.0	17.183 ± 0.005	18.510 ± 0.026	18.175 ± 0.013	18.301 ± 0.018
53 239.0	1.0	17.193 ± 0.006	18.508 ± 0.023	18.217 ± 0.014	18.317 ± 0.016
53 243.0	1.0	17.183 ± 0.007	18.502 ± 0.028	18.239 ± 0.015	18.298 ± 0.018

Table 3. (Contd.)

JD-2450000	FWHM	A	B	C	D
53 250.0	0.9″	17.143 ± 0.009	18.392 ± 0.034	18.120 ± 0.018	18.309 ± 0.022
53 253.0	1.2	17.212 ± 0.010	18.336 ± 0.022	18.157 ± 0.019	18.325 ± 0.023
53 257.0	1.1	17.196 ± 0.009	18.405 ± 0.019	18.148 ± 0.014	18.360 ± 0.021
53 259.0	0.9	17.193 ± 0.007	18.499 ± 0.015	18.291 ± 0.011	18.376 ± 0.016
53 266.0	1.3	17.188 ± 0.009	18.280 ± 0.031	18.133 ± 0.017	18.304 ± 0.023
53 268.0	1.0	17.198 ± 0.011	18.440 ± 0.026	18.228 ± 0.023	18.308 ± 0.027
53 289.0	1.2	17.199 ± 0.012	18.322 ± 0.028	18.126 ± 0.024	18.358 ± 0.022
53 292.0	1.0	17.192 ± 0.008	18.388 ± 0.016	18.216 ± 0.014	18.345 ± 0.018
53 297.0	1.1	17.200 ± 0.008	18.341 ± 0.017	18.197 ± 0.016	18.352 ± 0.022
53 300.0	1.3	17.188 ± 0.009	18.325 ± 0.023	18.148 ± 0.018	18.331 ± 0.026
53 307.0	0.9	17.239 ± 0.007	18.379 ± 0.015	18.273 ± 0.014	18.363 ± 0.018
53 309.0	0.9	17.192 ± 0.007	18.416 ± 0.021	18.139 ± 0.013	18.329 ± 0.014
53 320.0	1.1	17.197 ± 0.008	18.336 ± 0.018	18.198 ± 0.019	18.337 ± 0.021
53 527.0	1.1	17.188 ± 0.008	17.773 ± 0.020	18.158 ± 0.018	18.191 ± 0.038
53 528.0	1.0	17.196 ± 0.007	17.769 ± 0.016	18.188 ± 0.015	18.286 ± 0.032
53 535.0	1.1	17.190 ± 0.008	17.828 ± 0.020	18.150 ± 0.017	18.255 ± 0.029
53 536.0	1.0	17.225 ± 0.007	17.823 ± 0.018	18.264 ± 0.019	18.202 ± 0.027
53 537.0	1.0	17.221 ± 0.008	17.806 ± 0.019	18.176 ± 0.017	18.227 ± 0.031
53 541.0	1.1	17.229 ± 0.008	17.841 ± 0.021	18.181 ± 0.019	18.327 ± 0.035
53 542.0	1.1	17.219 ± 0.008	17.839 ± 0.020	18.217 ± 0.019	18.282 ± 0.035
53 544.0	1.3	17.246 ± 0.010	17.849 ± 0.028	18.142 ± 0.023	18.378 ± 0.042
53 545.0	1.7	17.223 ± 0.010	17.871 ± 0.029	18.104 ± 0.023	18.345 ± 0.034
53 551.0	1.1	17.199 ± 0.008	17.879 ± 0.021	18.194 ± 0.019	18.248 ± 0.033
53 552.0	1.0	17.243 ± 0.009	17.885 ± 0.024	18.193 ± 0.019	18.322 ± 0.043
53 554.0	1.1	17.240 ± 0.008	17.868 ± 0.019	18.244 ± 0.023	18.326 ± 0.026
53 555.0	1.2	17.233 ± 0.008	17.841 ± 0.020	18.240 ± 0.022	18.320 ± 0.021
53 556.0	0.9	17.282 ± 0.009	17.871 ± 0.016	18.265 ± 0.020	18.339 ± 0.019
53 557.0	1.0	17.283 ± 0.007	17.819 ± 0.017	18.276 ± 0.021	18.351 ± 0.017
53 558.0	1.2	17.225 ± 0.008	17.847 ± 0.024	18.327 ± 0.022	18.349 ± 0.024
53 559.0	1.3	17.184 ± 0.009	17.793 ± 0.023	18.246 ± 0.021	18.381 ± 0.023
53 564.0	1.0	17.269 ± 0.007	17.850 ± 0.017	18.294 ± 0.019	18.349 ± 0.019
53 565.0	1.1	17.255 ± 0.008	17.855 ± 0.021	18.296 ± 0.023	18.346 ± 0.020
53 566.0	1.2	17.253 ± 0.007	17.781 ± 0.022	18.260 ± 0.024	18.396 ± 0.023
53 569.0	1.1	17.264 ± 0.007	17.852 ± 0.019	18.302 ± 0.022	18.332 ± 0.019
53 570.0	1.1	17.272 ± 0.008	17.912 ± 0.017	18.319 ± 0.020	18.383 ± 0.016
53 571.0	1.0	17.299 ± 0.009	17.890 ± 0.017	18.288 ± 0.018	18.391 ± 0.023

Table 3. (Contd.)

JD-2450000	FWHM	A	B	C	D
53 577.0	1.0″	17.311 ± 0.007	17.919 ± 0.018	18.320 ± 0.021	18.393 ± 0.033
53 578.0	1.1	17.272 ± 0.009	17.924 ± 0.024	18.324 ± 0.025	18.335 ± 0.039
53 579.0	1.2	17.232 ± 0.008	17.892 ± 0.020	18.243 ± 0.023	18.392 ± 0.021
53 580.0	1.1	17.267 ± 0.007	17.940 ± 0.021	18.308 ± 0.021	18.389 ± 0.027
53 582.0	1.1	17.235 ± 0.009	17.942 ± 0.019	18.291 ± 0.024	18.309 ± 0.021
53 584.0	1.3	17.186 ± 0.010	17.898 ± 0.022	18.227 ± 0.018	18.263 ± 0.024
53 585.0	1.0	17.209 ± 0.007	17.925 ± 0.018	18.281 ± 0.023	18.292 ± 0.019
53 586.0	1.1	17.283 ± 0.009	17.881 ± 0.015	18.343 ± 0.027	18.308 ± 0.021
53 589.0	1.1	17.286 ± 0.008	17.864 ± 0.018	18.329 ± 0.033	18.332 ± 0.011
53 590.0	1.1	17.261 ± 0.005	17.860 ± 0.020	18.332 ± 0.019	18.365 ± 0.022
53 591.0	1.2	17.248 ± 0.008	17.869 ± 0.019	18.318 ± 0.026	18.349 ± 0.024
53 597.0	1.1	17.268 ± 0.007	17.854 ± 0.025	18.283 ± 0.028	18.319 ± 0.021
53 599.0	1.1	17.263 ± 0.010	17.905 ± 0.017	18.332 ± 0.021	18.361 ± 0.033
53 608.0	1.1	17.253 ± 0.007	17.916 ± 0.024	18.319 ± 0.019	18.315 ± 0.037
53 610.0	1.3	17.208 ± 0.012	17.904 ± 0.022	18.324 ± 0.019	18.292 ± 0.026
53 614.0	1.2	17.248 ± 0.008	17.918 ± 0.018	18.313 ± 0.022	18.311 ± 0.024
53 615.0	1.1	17.256 ± 0.006	17.907 ± 0.020	18.325 ± 0.025	18.270 ± 0.031
53 619.0	1.1	17.235 ± 0.011	17.916 ± 0.017	18.361 ± 0.029	18.277 ± 0.025
53 623.0	1.1	17.169 ± 0.013	17.884 ± 0.017	18.320 ± 0.021	18.305 ± 0.030
53 625.0	1.2	17.222 ± 0.007	17.879 ± 0.012	18.358 ± 0.016	18.326 ± 0.032
53 662.0	1.0	17.216 ± 0.005	17.871 ± 0.012	18.295 ± 0.021	18.311 ± 0.021
53 663.0	1.2	17.156 ± 0.015	17.891 ± 0.018	18.271 ± 0.029	18.331 ± 0.042
53 679.0	1.0	17.146 ± 0.007	17.853 ± 0.016	18.254 ± 0.019	18.345 ± 0.018
53 703.0	1.4	17.145 ± 0.008	17.835 ± 0.013	18.214 ± 0.022	18.355 ± 0.026
53 704.0	1.6	17.128 ± 0.011	17.832 ± 0.025	18.221 ± 0.032	18.349 ± 0.043
53 705.0	1.0	17.171 ± 0.011	17.816 ± 0.026	18.254 ± 0.034	18.344 ± 0.045

measured magnitudes as the rms deviations from the mean in the series divided by the square root of the number of frames in the series.

The most prominent event in the system in the period considered was appreciable brightness variations of component B. In 2000, component B was the faintest component in the system. However, substantial brightness variations are observed in 2004–2005, with the component's brightness maximum reached in May 2005. On average, the magnitude of component B varied by 0.9^m. The duration of this event was ~300 days. The observations for the end of 2005 show that the brightness of component B had returned to its level in 2004. The brightness increase for component B in 2004–2005 was monotonic. The 2005 observing season began immediately after the component reached its maximum brightness. The brightnesses of components C and D varied only slightly in this period.

Substantial variations in the brightness of one of the components can occur when the source passes near or directly across a caustic [21], with the increase in brightness reaching a substantial fraction of a magnitude. The theoretical calculations of [22] show that the color variations that occur during microlensing are correlated with the brightness vari-

Table 4. $V-R$ and $V-I$ color indices for components A and B of Q2237 + 0305 derived from the 2004–2005 Maidanak Observatory data

JD-2450000	Component A		Component B	
	$V-R$	$V-I$	$V-R$	$V-I$
53 171.0	0.072 ± 0.011	0.209 ± 0.019	0.242 ± 0.015	0.412 ± 0.016
53 202.0	0.130 ± 0.010	0.263 ± 0.018	0.236 ± 0.012	0.436 ± 0.021
53 232.0	0.094 ± 0.006	0.244 ± 0.011	0.243 ± 0.014	0.428 ± 0.017
53 260.0	0.155 ± 0.009	0.303 ± 0.010	0.236 ± 0.026	0.377 ± 0.016
53 294.0	0.158 ± 0.009	0.305 ± 0.006	0.201 ± 0.016	0.369 ± 0.013
53 539.0	0.125 ± 0.007	0.321 ± 0.009	0.176 ± 0.015	0.217 ± 0.012
53 568.0	0.132 ± 0.008	0.342 ± 0.009	0.121 ± 0.011	0.215 ± 0.013
53 599.0	0.117 ± 0.009	0.347 ± 0.011	0.151 ± 0.012	0.219 ± 0.014
53 620.0	0.113 ± 0.012	0.331 ± 0.022	0.157 ± 0.013	0.210 ± 0.017
53 662.0	0.117 ± 0.021	0.307 ± 0.019	0.187 ± 0.029	0.223 ± 0.024

Table 5. $V-R$ and $V-I$ color indices for components C and D of Q2237 + 0305 derived from the 2004–2005 Maidanak Observatory data

JD-2450000	Component C		Component D	
	$V-R$	$V-I$	$V-R$	$V-I$
53 171.0	0.153 ± 0.019	0.341 ± 0.036	0.165 ± 0.023	0.322 ± 0.041
53 202.0	0.160 ± 0.011	0.331 ± 0.019	0.187 ± 0.014	0.352 ± 0.027
53 232.0	0.173 ± 0.012	0.320 ± 0.021	0.146 ± 0.013	0.317 ± 0.015
53 260.0	0.189 ± 0.023	0.345 ± 0.028	0.169 ± 0.016	0.340 ± 0.025
53 294.0	0.197 ± 0.024	0.371 ± 0.034	0.177 ± 0.017	0.371 ± 0.026
53 539.0	0.131 ± 0.037	0.349 ± 0.018	0.161 ± 0.015	0.393 ± 0.022
53 568.0	0.212 ± 0.016	0.396 ± 0.017	0.211 ± 0.010	0.404 ± 0.021
53 599.0	0.167 ± 0.017	0.399 ± 0.019	0.184 ± 0.016	0.395 ± 0.021
53 620.0	0.191 ± 0.015	0.402 ± 0.029	0.179 ± 0.014	0.391 ± 0.038
53 662.0	0.182 ± 0.027	0.398 ± 0.014	0.167 ± 0.024	0.401 ± 0.036

ations. Substantial variations in the colors of the components and a tendency for the components to become bluer as they brighten can be noted for the microlensing events for components A and C in 1999. The colors for all four components and their variations based on observations made in 1995–2000 are presented in [5]. Analysis of the brightness and color variations of the components reveals a correlation between the $V-I$ color index and brightness variations.

It is possible to characterize the microlensing event for component B using detailed numerical modeling. A comparative analysis with the previous events in components A and C is also possible. Figure 3 presents the variations of the mean $V-I$ color index of component B for each month of observations in 2004–2005 and for the microlensing events for components A and C in 1999. The curves are shifted so that their maxima occur at time $t = 0$. The color-index variations for components A and C from 1997 to 2000 are presented in [5]. The color-index variations

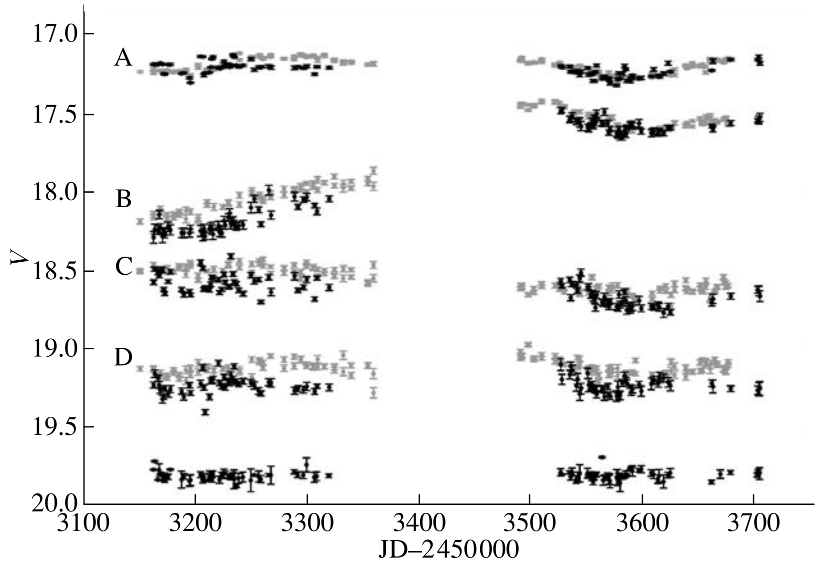

Fig. 2. V light curves of the components of the Q2237+0305 system based on the 2004–2005 Maidanak Observatory data. The light curve of a comparison star is shown in bottom. The V light curves of the components obtained by the OGLE group for the same observing period are shown in gray.

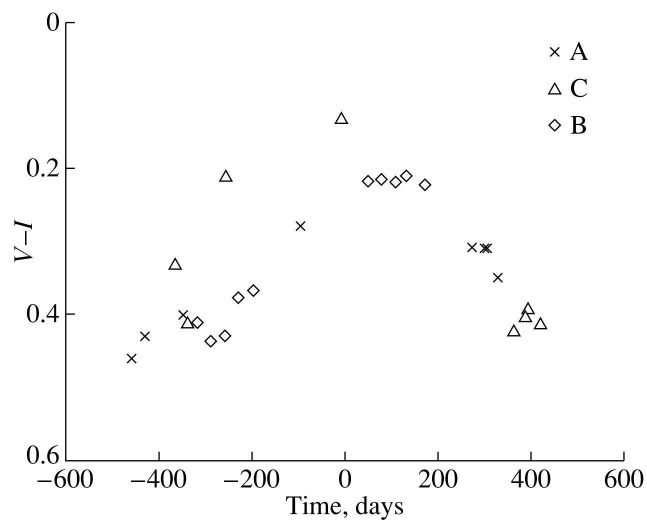

Fig. 3. $V-I$ color light curves for the microlensing events for components A and C of the Q2237+0305 in 1999 and for the peak of component B in May 2005. The curves are shifted so that they have their maxima at time $t = 0$.

for component C were symmetrical about the maximum. A high degree of symmetry is also observed for the brightness variations. This led some groups to interpret these variations as the passage of the source near the cusp of a caustic [23]. On the contrary, the microlensing event for component A was interpreted as the source crossing a caustic line [24]. The $V-I$ color index for component A varied by 0.15^m, while the component's magnitude varied by 0.45^m. The color index did not return to its value at the onset of the microlensing event. Analysis of observations for 2004–2005 showed that the $V-I$ color index for component B varied by 0.2^m, and did not return to its value in Autumn 2004. However, the components' light curves based on subsequent observations of the system, including 2006 observations by the OGLE group [25], were not able to confirm the hypothesis that component B underwent a microlensing event associated with a caustic crossing.

5. CONCLUSION

We have presented the results of a photometric reduction of images of the gravitationally lensed system Q2237+0305 (Tables 3, 4, 5). The input observational material was obtained on the 1.5-m telescope of the Maidanak Observatory. We used the algorithm described in [15] for the photometric measurements. All of our calculations were carried out using a numerical model for the lensing galaxy obtained with a regularization method, assuming that the brightness distribution of the galaxy was close to an analytical profile [17, 18]. This yielded new data on the variability of the components of Q2237+0305 in V, R, and I during 2004–2005. Our analysis of the resulting light curves revealed substantial brightness variations of component B (by 0.9^m), with their maximum in May 2005. These brightness variations were also accompanied by color variations (Table 4 and Fig. 3).

The very first multi-color observations of the system [10] showed that the components have different colors. Variations of the component colors relative to these first multi-color observations were later noted in [2, 26]. VRI photometric data obtained on the NOT [3] showed that the colors of the pairs (A, B) and (C, D) are approximately the same, with the difference between the pairs in V being $\sim 0.6^m$. It was then reported in [11, 14] that component B had become bluer since the first observations in 1987. An attempt to analyze the color variations in the Q2237+0305 system was made in [27, 28], using V, R, and I data obtained on the 1.5-m Maidanak Observatory telescope in 1997–1998. Appreciable color variations of the components and a tendency for the components to become bluer as they brighten were noted. An analysis of the collected multi-color photometric data for 1995–2000 [5] showed the presence of a correlation between the color and brightness variations of the components.

Three main possible origins for the color variations of the components of the gravitationally lensed system have been considered: a time delay between the components light curves compared at a given epoch, absorption in the lensing galaxy, and microlensing by stars in the lensing galaxy. Since the time delay between the components of Q2237+0305 is about one day, brightness variations occurring in the source should appear nearly simultaneously in all four components. The first report of correlated brightness variations for the components was made in [3]. Correlated brightness variations in at least three of the components were also observed in 2003 [29, 30]. Based on the assumption that these represented intrinsic variability of the quasar, Koptelova et al. [30] estimated the time delay between the variations in V and R filters. However, the light curves for all four components obtained by various groups clearly demonstrate that the system is characterized by brightness variations that are completely uncorrelated. Thus, the main variations in the system are due to microlensing by stars in the lensing galaxy. Since the most probably variations are associated with microlensing, analysis of microlensing events appears to be the only means of investigating the system.

Multi-color observations of the system during microlensing events with high amplifications can be used to estimate the size of the radiating region of the quasar at various wavelengths [22]. Model computations based on data for a microlensing event in component A in 1999 obtained by the OGLE group [32] and the upper limit derived for the transverse velocity of the stars in the galaxy [31] made it possible to place limits on the size of the source in V and R wavebands. Applying a non-parametric method for reconstructing the source to the observational data for the microlensing event in component A yielded the brightness distribution of the source [33].

Another possible origin of brightness variations of the components is absorption in the lensing galaxy [34]. Both variations in the galactic absorption and the effects of microlensing could lead to time variations of the colors of the components. Separating the effects of these two mechanisms giving rise to color variations in the components is very difficult. Regular multi-color monitoring observations of the system are essentially for studies of these two mechanisms and attempts to distinguish between their contributions to color variations of the components.

ACKNOWLEDGMENTS

This work was supported by a Presidential Grant of the Russian Federation for the Support of Young Russian Scientists (MK-2637.2006.2) and the Russian Foundation for Basic Research (project codes 05-01-00049, 05-02-16454, and 06-02-16857).

REFERENCES

1. J. Huchra, M. Gorenstein, S. Kent, et al., Astron. J. **90**, 691 (1985).
2. R. T. Corrigan, M. J Irwin, J. Arnaud, et al., Astron. J. **102**, 34 (1991).
3. R. Østensen , S. Refsdal, R. Stabell, et al., Astron. Astrophys. **309**, 59 (1996).
4. D. Alcalde, E. Mediavilla, O. Moreau, et al., Astrophys. J. **572**, 729 (2002).
5. V. G. Vakulik, R. E. Schild, V. N. Dudinov, et al., Astron. Astrophys. **420**, 447 (2004).
6. E. Koptelova, E. Shimanovskaya, B. Artamonov, et al., Mon. Not. R. Astron. Soc. **356**, 323 (2005).
7. M. J. Irwin, R. L. Webster, P. C. Hewett, et al., Astrophys. J. **98**, 1989 (1989).

8. P. R. Wozniak, C. Alard, A. Udalski, et al., Astrophys. J. **529**, 88 (2000).
9. P. R. Wozniak, A. Udalski, M. Szymanski, et al. Astrophys. J. **540**, L65 (2000).
10. H. K. C. Yee, Astron. J. **95**, 1331 (1988).
11. I. Burud, R. Stabell, P. Magain, et al., Astron. Astrophys. **339**, 701 (1998).
12. P. Magain, F. Courbin, and S. Sohy, Astrophys. J. **494**, 472 (1998).
13. C. Alard and R. H. Lupton, Astrophys. J. **503**, 325 (1998).
14. V. G. Vakulic, V. N. Dudinov, A. P. Zheleznyak, et al., Astron. Nachr. **318**, 73 (1997).
15. E. Koptelova, E. V. Shimanovskaya, B. P. Artamonov, et al., Astron. Rep. **48**, 826 (2004).
16. A. Belokurov, E. V. Shimanovskaya, M. V. Sazhin, et al., Astron. Zh. **78**, 876 (2001) [Astron. Rep. **45**, 759 (2001)].
17. E. Koptelova, E. Shimanovskaya, B. Artamonov, et al., in *Gravitational Lensing: a Unique Tool for Cosmology*, Ed. by D. Valls-Gabaud and J. P. Kneib, Astron. Soc. Pac. Conf. Ser. **326**, 45 (2003); astro-ph/0311508.
18. A. Yagola, B. Artamonov, V. Belokurov, et al., in *Inverse Problems in Engineering Mechanics IV,* Ed. by M. Tanaka (Elsevier, 2003).
19. J. A. Hogbom, Astron. Astrophys., Suppl. Ser. **15**, 417 (1974).
20. R. Østensen, Candidata Scientarium Thesis (Univ. of Tromsø, 1994).
21. A. F. Zakharov, *Gravitational Lenses and Microlenses* (Yanus, Moscow, 1997) [in Russian].
22. J. Wambsganss and B. Paczinski, Astrophys. J. **102**, 864 (1991).
23. J. S.B. Wyithe, R. L. Webster, and E. L. Turner, Mon. Not. R. Astron. Soc. **315**, 51 (2000).
24. R. Gil-Merino, J. González-Cadelo, L. J. Goicoechea, et al., Mon. Not. R. Astron. Soc. **371**, 1478 (2006); astro-ph/0607162.
25. A. Udalski, M. K. Szymański, M. Kubiak, et al., astro-ph/0701300v1 (2007).
26. H. W. Rix, D. P. Schneider, and J. N. Bachall, Astron. J. **104**, 959 (1992).
27. V. N. Dudinov, V. G. Vakulik, A. P. Zheleznyak, et al., Kinematika Fiz. Nebesnykh Tel **16**, 346 (2000).
28. V. N. Dudinov, P. Bliokh, P. Pachinskii, et al., Kin. Fiz. Neb. Tel **3**, 170 (2000).
29. V. Vakulik, R. Schild, V. Dudinov, et al., Astron. Astrophys. **447**, 905 (2006).
30. E. Koptelova, V. Oknyanskij, and E. Shimanovskaya, Astron. Astrophys. **552**, 37 (2006).
31. J. S.B. Wyithe, R. L. Webster, and E. L. Turner, Mon. Not. R. Astron. Soc. **309**, 261 (1999).
32. V. N. Shalyapin, L. J. Goicoechea, D. Alcalde, et al., Astrophys. J. **579**, 127 (2002)
33. M. G. Bogdanov and A. M. Cherepashchuk, Astron. Zh. Astron. Rep. **46**, 626 (2002).
34. D. Nadeau, H. K.C. Yee, W. J. Forrest, et al., Astrophys. J. **376**, 430 (1991).

Translated by D. Gabuzda